

An infrared proper motion study of the Orion bullets

J.-K. Lee^{*} and M. G. Burton

School of Physics, University of New South Wales, Sydney, NSW 2052, Australia

Submitted: 3 August 1999

ABSTRACT

We report the first IR proper motion measurements of the Herbig-Haro objects in the Orion Molecular Cloud–One using a four-year time baseline. The [Fe II] emitting bullets are moving of order 0.08 arcsec per year, or at about 170 km s^{-1} . The direction of motion is similar to that inferred from their morphology. The proper motions of H_2 emitting wakes behind the [Fe II] bullets, and of newly found H_2 bullets, are also measured. H_2 bullets have smaller proper motion than [Fe II] bullets, while H_2 wakes with leading [Fe II] bullets appear to move at similar speeds to their associated bullets. A few instances of variability in the emission can be attributed to dense, stationary clumps in the ambient cloud being overrun, setting up a reverse-oriented bullet. Differential motion between [Fe II] bullets and their trailing H_2 wakes is not observed, suggesting that these are not separating, and also that they have reached a steady-state configuration over at least 100 years. The most distant bullets have, on average, larger proper motions, but are not consistent with free expansion. Nevertheless an impulsive, or short-lived ($\ll 1,000$ years) duration for their origin seems likely.

Key words: ISM: jets and outflows, ISM: infrared

1 INTRODUCTION

The Orion Nebula (M42, NGC 1976) is the nearest massive star forming region, at a distance of 450 pc (Genzel & Stutzki 1989), thus becoming the archetype for studying related phenomena such as outflows, shocks and photodissociation. A score of planetary-mass ‘bullets’ were discovered in the core of Orion Molecular Cloud–One (OMC–1) by Allen & Burton (1993, AB hereafter). The bullets are prominent in near-IR [Fe II] $a^4F_{5/2} - a^4D_{7/2}$ $1.64 \mu\text{m}$ line emission, with trailing wakes bright in H_2 1-0 S(1) $2.12 \mu\text{m}$ line emission, which are sensitive to intermediate ($\geq 50 \text{ km s}^{-1}$) and slow ($\leq 50 \text{ km s}^{-1}$) speed shocks, respectively. The bullets were identified with fast moving optical Herbig–Haro (HH) objects observed by (?) in the [O I] 6300\AA line. As indicated by their line widths, they are travelling out of the cloud at speeds of up to 400 km s^{-1} . Projecting back, the wakes point to an origin within 5 arcsec of the IRc2–complex. Their dynamical age is no more than 1,000 years. A second finger system was found by Stolovy et al. (1998) from HST/NICMOS observations, within ≈ 15 arcsec of the IRc2–complex. This inner finger system emits in H_2 only, with no [Fe II] emission at their tips. These bullets are presumably interacting at lower speeds with the medium, leading to a lower-excitation spectrum.

The formation mechanism for these bullet systems is not yet clearly understood. Two competing hypothesis are 1) one or multiple explosive events fling off ejecta from the IRc2–complex (AB) and 2) *in situ* Rayleigh–Taylor instabilities in time-variable winds, or in a slow wind being overtaken by faster moving wind (Stone et al. 1995). A proper motion study can verify the bow shock interpretation of the bullet-wake systems. If motions are not detected, perhaps because the emission arises in a standing wave in the flow of a wind from a central source, the ejection model (AB) would be invalid. Together with line profile measurements, proper motions may constrain the location of the central source by determining the three dimensional structure and velocities. In addition, relative proper motions of the H_2 and [Fe II] gas in a wake and bullet provide constraints on how ambient material is entrained by the leading bullet.

Previously Jones & Walker (1985) measured the proper motion of three optical bullets (HH 201, 205 and 210, following the nomenclature of Reipurth 1999) by comparing 20 plates, all taken on infrared emulsion (1–N or 103a–U) through an RG-8 (\equiv RG–695) filter with the Lick Observatory 120-inch telescope between 1960 and 1983. They showed large tangential velocities, and the authors speculated that the sources IRc2 and IRc9 must be responsible for the excitation, residing at most ~ 0.2 pc behind an obscuring molecular cloud. Hu (1996) used narrow band [N II] 6583\AA images taken by HST/WFPC with a 4 year baseline to also de-

^{*} email: jklee@phys.unsw.edu.au

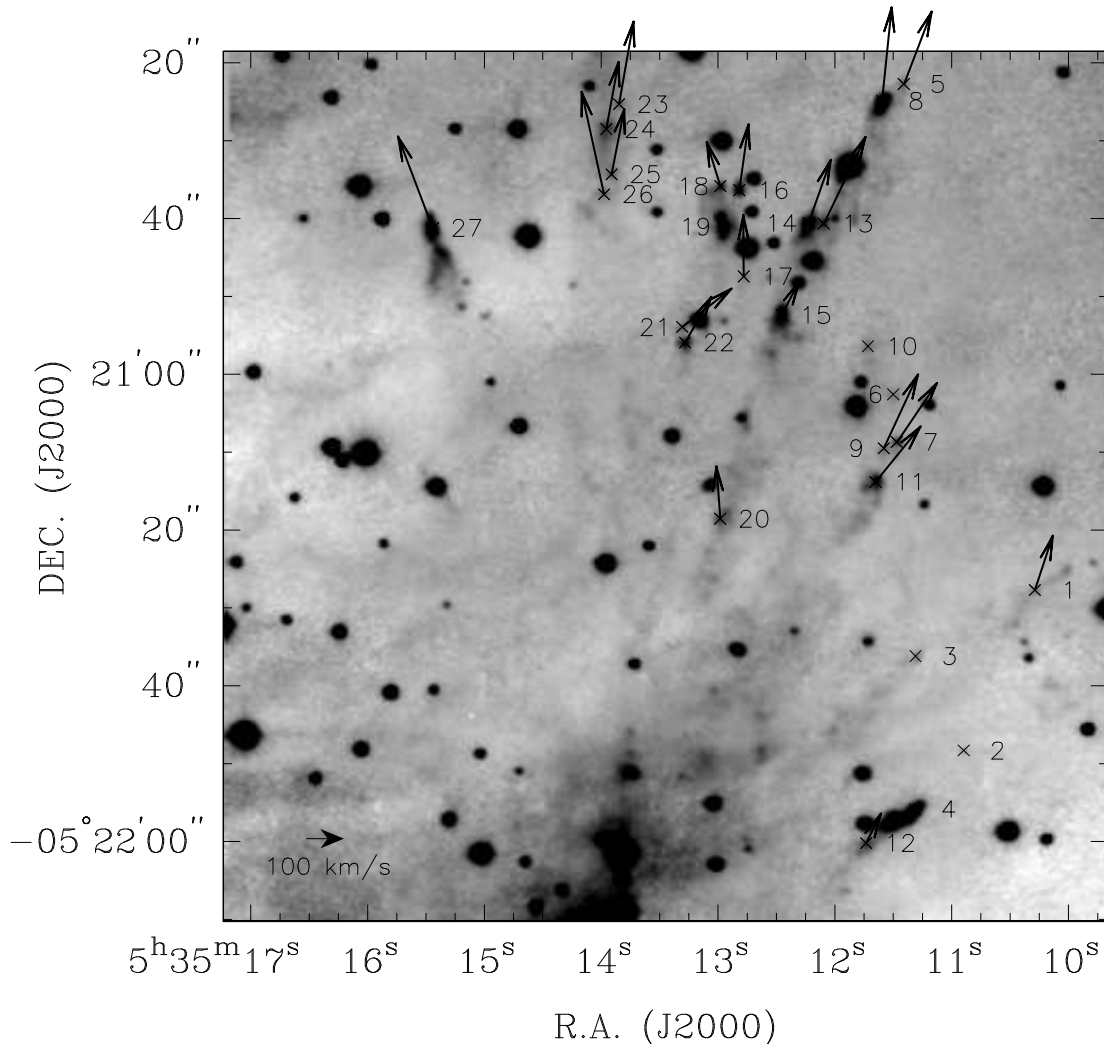


Figure 1. The [Fe II] $1.64 \mu\text{m}$ image of OMC-1 taken in December 1996, with proper motion vectors from the centroid method overlaid. For HH 117-200 (No.12) and HH 130-119 (No.20) the proper motion vectors from eye-estimation are used (see §3.1). The length and orientation of an arrow represents the transverse speed of a bullet and its direction of motion. A scale bar in the lower left corner corresponds to a speed of 100 km s^{-1} at a distance of 450 pc and its length to the distance a bullet would cover in 100 years. The IRc2-complex, where the driving source is presumed to be located, is at $5^{\text{h}}35^{\text{m}}14^{\text{s}}.4$, $-5^{\circ}22'30''$ (J2000), below the image. Every bullet whose proper motion has been measured is numbered (first column of Table 1). Those whose motion has $S/N < 3$ are marked with a cross only.

termine their proper motions, and long-slit, high resolution echelle spectra of [O I] in measuring the three dimensional kinematics. He estimated shock velocities and orientation angles for HH 201, 205, 206 and 210 adopting the bow shock model and analysis by Hartigan et al. (1987). He suggested that a hydrodynamic instability in a shell swept up by a poorly collimated stellar wind from young stars is responsible for the formation of these objects.

Through high resolution spectroscopic observations of the [Fe II] $1.64 \mu\text{m}$ line, Tedds et al. (1999a) obtained line profiles for the bullets HH 126-053 (=HH 207; here HH 125-053, see text) and HH 120-114 (here HH 117-114). From the shape of the integrated [Fe II] line profiles, they derived the bullet velocity and the orientation angle based on the analysis of Hartigan et al. (1987) that showed the full-width zero intensity (FWZI) of the integrated profile over a single bow shock must be equal to the speed of the bullet itself. The re-

sults from these studies are give in Table 1 for comparison. We have used images of the [Fe II] and H_2 lines, taken during periods of exceptional seeing and with a 4-year baseline, to investigate proper motions of the multitude of bullets which are observable at near-IR wavelengths.

Data acquisition and analysis is presented in Section 2, with the results from this and previous studies in Section 3. Discussion and plans for future work are followed in Section 4 and 5, respectively.

2 OBSERVATIONS & DATA ANALYSIS

A region of $\sim 2 \times 2$ arcmin in OMC-1 was mapped in 1992 September 13 and 1996 November 24, giving a 4.2 year time baseline, with the IRIS near-IR camera (Allen et al. 1993) on the 3.9-m Anglo-Australian Telescope. Narrow-band line

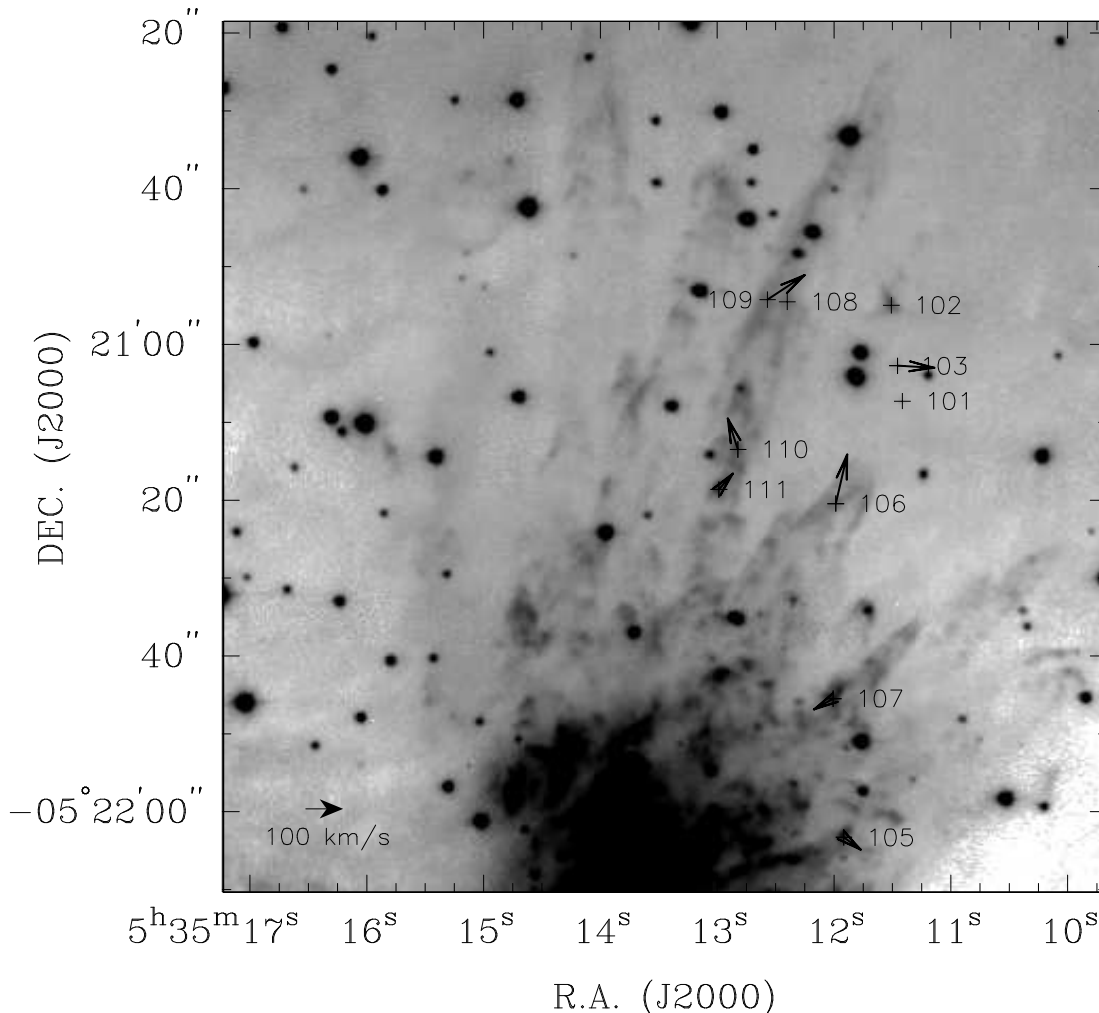


Figure 2. The H₂ 1–0 S(1) 2.12 μm image of OMC–1 taken in December 1996, with proper motion vectors overlaid as Figure 1. A newly found H₂ bullet HH 117–212 (No. 104) is out of the frame and not shown. For its location, see Figure 6. Every H₂ knot whose proper motions have been measured is numbered (first column of Table 1). Those with $S/N < 3$ are marked with a plus sign (+) only.

images in [FeII] 1.64 μm and H₂ 2.12 μm emission were taken with 30 second integration time. A pixel scale of 0.27 arcsec was used for both data sets with sub-arcsecond seeing (0.7'' in 1992 and 0.9'' in 1996) for both epochs. The data reduction process involved the usual bad pixel removal, flat-fielding and sky subtraction. A slight field rotation (12.2') between the two epochs was corrected for the second epoch data with a transformation solution obtained by using common stars in the field. The error involved in image registration is of order a tenth of a pixel. We did not attempt to correct for different seeing between the epochs.

Since the bullets and trailing wakes are diffuse objects, their proper motion depends on whether one is measuring their bulk motion, and/or viewing changes in morphology as well. We adopted three methods which are sensitive to different aspects of motion; 1) image centroiding, 2) cross-correlation and 3) eye-estimation. Centroiding is sensitive to motion of the emission centroid of an object, and cross-correlation to morphological changes. A small area of sky around an object is selected in two epochs and cross-correlated, producing a resultant image. The amount of shift

of the peak intensity from the centre in this cross-correlated image was interpreted as proper motion. In reality, however, it reflects both bulk motion and changes in shape of the object. If the results from the first two methods do not agree, we attributed this to morphological changes, which was often confirmed by the third method – eye examination. Contours of the object in two epochs were compared by eye to give the shift in the position of intensity peaks only.

In naming a bullet, we followed the nomenclature proposed by O'Dell & Wen (1994) to designate compact sources and stars in M42. It assigns to an object a catalog number indicating the position of the source. The first three digits indicate the position in right ascension (E2000), and the second three the position in declination. The common values for the inner region of M42 ($5^{\text{h}}35^{\text{m}}$ and $-5^{\circ}20'$) are not included. Hence, a bullet located at $5^{\text{h}}35^{\text{m}}11^{\text{s}}51$, $-5^{\circ}21'47''$ would become 115-147. The coordinates of PC043, $5^{\text{h}}35^{\text{m}}13^{\text{s}}39$, $-5^{\circ}21'08.0''$, from a HST WF/PC survey (Prosser et al. 1994) was used as the reference position to obtain the coordinates of bullets.

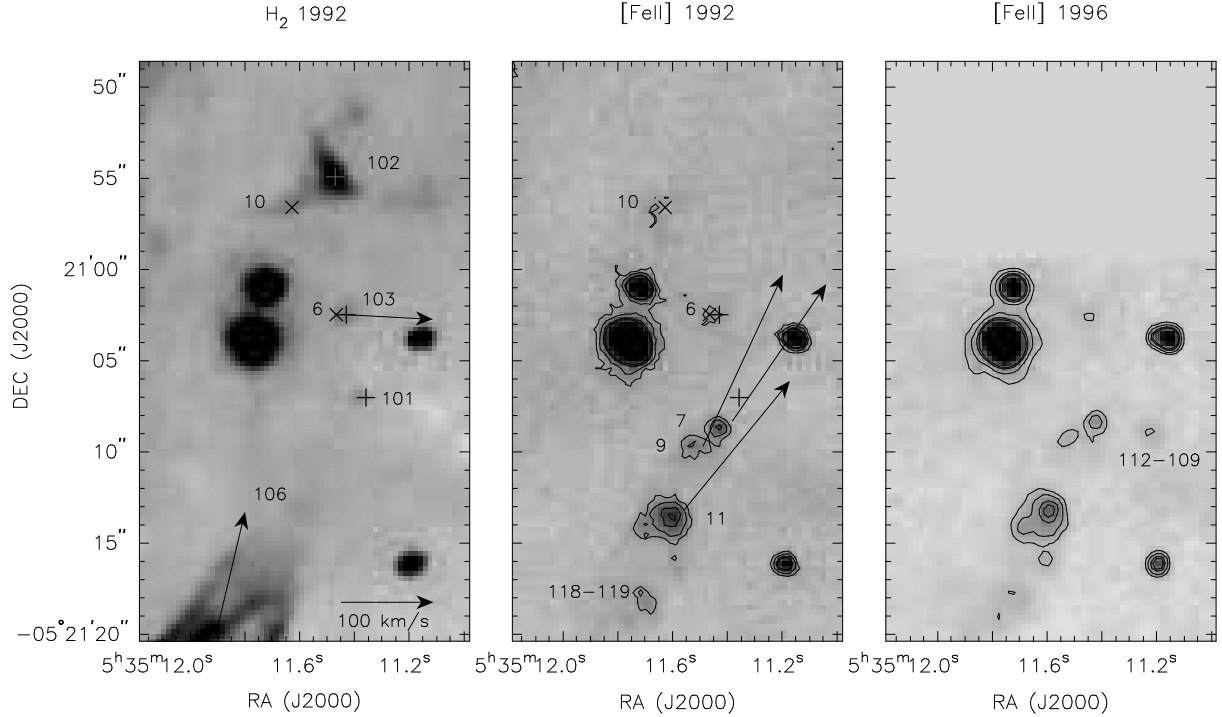


Figure 3. Enlarged images around HH 117-114 of H₂ in 1992 (*left*), [Fe II] in 1992 (*centre*) and [Fe II] in 1996 (*right*). The compact [Fe II] emission knot, HH 117-114 (No. 11), lies at the head of wakes in H₂. Two more [Fe II] bullets, HH 115-109 (No. 7) and HH 116-110 (No. 9) are in front of it. A stationary clump 114-107 (No. 101) in H₂ emission lying ahead of them. Presumably it is being rammed by the HH 115-109/HH 117-114 (Nos. 7/11) bullet system. An [Fe II] clump shows up as HH 112-109 only in 1996, and was not seen in 1992 (middle and right panels). HH 117-057 (No. 10) is stationary, accompanied by a bright triangle-shaped stationary H₂ clump, 115-055 (No. 102) next to it. The velocity vector and the scale bar, on the left panel, is the same as in Figure 1. H₂ knots are marked by + and [Fe II] knots by ×.

3 RESULTS

The results of the proper motion measurements of the Orion bullets and wakes are listed in Table 1 (see also Figure 1 for [Fe II] and Figure 2 for H₂), as well as the results from previous studies. The average proper motion of [Fe II] bullets and their trailing H₂ wakes is about 8 arcsec per century for those whose proper motion has been measured, corresponding to a transverse speed of 170 km s^{-1} at the distance of 450 pc to OMC-1. For bullets whose motion has $S/N \geq 3$, the average proper motion is 9.4 arcsec per century with a corresponding transverse speed of 200 km s^{-1} . The direction is similar to that inferred from their morphology. In general, the three methods have given similar results (aside from HH 109-148, HH 113-156 and HH 130-041) as there are few clear changes in the bullet morphology over the 4 year baseline. However some bullets and wakes have change in shape and/or intensity, as described below. We first discuss the proper motions seen in the [Fe II] images, and then in the H₂ images.

3.1 Noticeable Features in [Fe II] Line Emission

Features for individual [Fe II] bullets are described below in the ascending order of their R.A. coordinate. Their designation from the previous studies are also given in parenthesis when available, and the number following is from Column 1 in Table 1.

HH 113-156 (=HH 201) & HH 117-200 [Nos. 4 & 12]

This shows a double feature and/or unresolved substructure within it, ~ 1.5 arcsec, or ~ 600 AU in size. O’Dell & Wong (1996) identified this as four separate objects of 113-153, 114-155, 155-155 and 116-156. It has no counterpart or wake in H₂, attributed to its motion close to our line of sight. Different methods give different proper motion values, mainly due to its double feature and unsymmetric shape. The tangential velocity v_{tan} calculated from centroiding, $38 \pm 21 \text{ km s}^{-1}$, disagrees with those from previous studies. This probably results from partially resolving the feature into two components. v_{tan} obtained from cross-correlation (177 km s^{-1}) and from eye-estimation (100 km s^{-1}) both agree reasonably. They give an orientation angle (O.A.) of 60° for the former, and 20° for the latter method when combined with Hu (1996)’s estimation of the shock velocity 310 km s^{-1} . O.A. is the angle between the direction of motion of an object in space and our line-of-sight.

HH 117-200 (No. 12) shows weak [Fe II] emission, located just southeast of HH 113-156 (No. 4), however their association is not clear. The proper motion determined for HH 117-200 (No. 12) vary for different methods; centroiding gives a motion to the northeast with P.A.= 30° while the other two methods to the northwest with P.A.= 330° . Its v_{tan} also varies from 90 km s^{-1} (eye-estimation) to 213 km s^{-1} (cross-correlation). Its overall intensity distribution remains the same for both epochs, and a small shift in emis-

sion peak is attributed as the cause of this discrepancy.

HH 115-109/HH 117-114 (=HH 120-114)

[Nos. 6, 7, 9, 10 & 11]

This bullet system was designated as HH 120-114 by Tedds et al. (1999a) (without exact astrometry) using AB's 1992 image, but we separate them into two (possibly three or more, see below) bullets with clear evidence of a double feature in the H₂ wakes behind them (Figure 3). The bullets are moving at a similar speed of $\sim 200 \text{ km s}^{-1}$ and position angle of 320° . HH 116-110 (No. 9), a secondary emission peak in the [Fe II] wake of HH 115-109 (No. 7), moves slightly faster than HH 115-109 (No. 7). It is not clear whether they are separate bullets. Tedds et al. (1999a) derived the bullet velocity and O.A. for this system from the shape of the integrated [Fe II] profiles. They derived a shock velocity $v_s = 120 \pm 10 \text{ km s}^{-1}$ and O.A. = $60 \pm 15^\circ$ giving a corresponding v_{tan} of $100 \pm 25 \text{ km s}^{-1}$. The difference in v_{tan} from that derived here indicates that using the shape of line profiles to infer orientation angles can be unreliable. In this particular case several profiles are overlapping.

A knot at 115-103 (No. 6/103) shows weak emission in both [Fe II] and H₂ lines with a slight offset. Both species show similar proper motions of 100 km s^{-1} . Note the proper motion in [Fe II] from eye-estimation is greater than that from centroiding, due to a small shift in emission peak to west. HH 117-057 (No. 10) is found to be stationary next to a bright H₂ clump 115-055 (No. 102). From the relative locations of [Fe II] and H₂, we suggest that this is a 'reverse' bullet, i.e. a dense, stationary condensation being rammed by outflowing material, producing a reverse-oriented bow shock (see §4).

The proper motion of a knot at 118-119 was not measurable because it lies in the middle of diffuse [Fe II] emission in the tail of the HH 115-109/HH 117-114 (Nos. 7/11) system. In addition the weak emission peak in 1992 had become more diffuse by 1996. Interestingly it lies along the axis of one of the following H₂ wakes, suggesting this is more directly associated with them (see §3.2). Note an [Fe II] clump which showed up at 112-109 in 1996 (Figure 3). It was not seen in 1992 indicating intensity variability.

HH 116-025, HH 122-041 & HH 125-053 (=HH 205, HH 206 & HH 207) [Nos. 5, 8, 13, 14 & 15]

This is the most crowded field with several bullets and wakes overlapping (Figure 4). Thus this field is suitable for determining whether any differential motion between bullets and/or between species occurs, i.e. whether or not the bullets move with different speeds depending on their distance from the origin, and/or if their H₂ wakes are stretching out behind them. However, no differential motion was detected. This may be attributable to the short time baseline. If such motion was, for example, 30 km s^{-1} , a 10-year baseline would be required.

HH 116-025 (=HH 205, No. 8) is one of the fastest moving bullets ($\sim 250 \text{ km s}^{-1}$) at the tip of the most crowded finger. Hu (1996) reported a morphological change in [N II], but no change is apparent in our [Fe II] image. His estimation of $v_s = 310 \text{ km s}^{-1}$ with O.A. = 90° (moving on the plane-of-sky), makes the expected tangential velocity the same as the shock velocity. A smaller bullet, HH 114-023 (No. 5), located further northwest of it, shows similar proper motion.

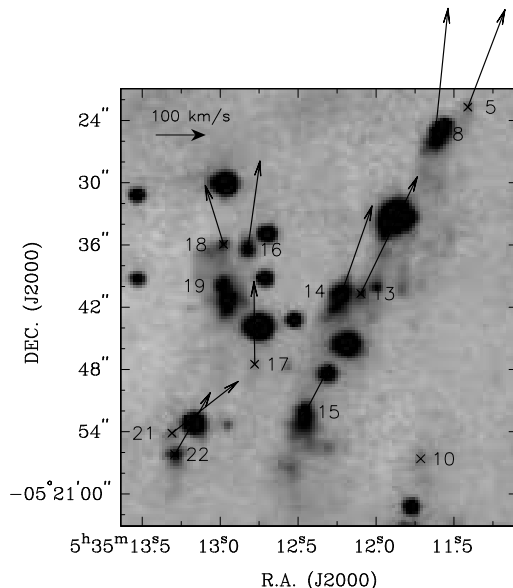


Figure 4. A blow-up of the most crowded field accommodating HH 116-025, HH 122-041 and HH 125-053 (Nos. 8, 14 & 15). The velocity vector and the scale bar, at the upper left corner, are the same as in Figure 1.

HH 122-041 (No. 14) is irregular in shape having the same direction of motion with HH 116-025 and HH 125-053 (Nos. 8 & 15). For HH 125-053 (=HH 207, HH 126-053; No. 15), $\sim 100 \text{ km s}^{-1}$ proper motion is measured while the estimation by Tedds et al. (1999a) gives $v_{tan} = 140 \pm 25 \text{ km s}^{-1}$, with $v_s = 150 \pm 10 \text{ km s}^{-1}$ and O.A. = $70 \pm 15^\circ$. Emission at the bullet head is observed to get stronger without any morphological change.

HH 130-119 [No. 20]

HH 130-119 is located along the line of a series of prominent bullets; HH 116-025, 122-041 and 125-053 (Nos. 8, 14 and 15, respectively). It is quite diffuse in shape with no noticeable emission peak in the 1992 image. In 1996, however, an emission peak was prominent in the lower-left corner of the bullet, considerably affecting the proper motion measurement using image centroid and cross-correlation. By blinking between two epoch data, we can see its motion toward northwest (P.A. = 5°), and this value is used in Figure 1. This demonstrates the limitation of centroiding when a bullet changes its intensity distribution over time. Apparently it has the largest proper motion, but this is a reflection of the change in distribution within its diffuse, irregular morphology, rather than of actual bulk motion.

HH 154-041 (=HH 210) [No. 27]

Jones & Walker (1985) reported a 'nucleus' in its head. We also see this in [Fe II] and in J band ($1.25 \mu\text{m}$), as much fainter emission with similar morphology, but not in H₂ emission. This could mean that its motion is close to our line of sight, or that it has escaped from the molecular cloud, hence no H₂. While zero proper motion was expected from Hu (1996)'s estimation of $v_s = 400 \text{ km s}^{-1}$ and O.A. = 0° (moving directly toward us), our measurement gives $v_{tan} = 260 \text{ km s}^{-1}$. In fact, the morphology suggests there are at least two bow features overlapping – while the overall shape

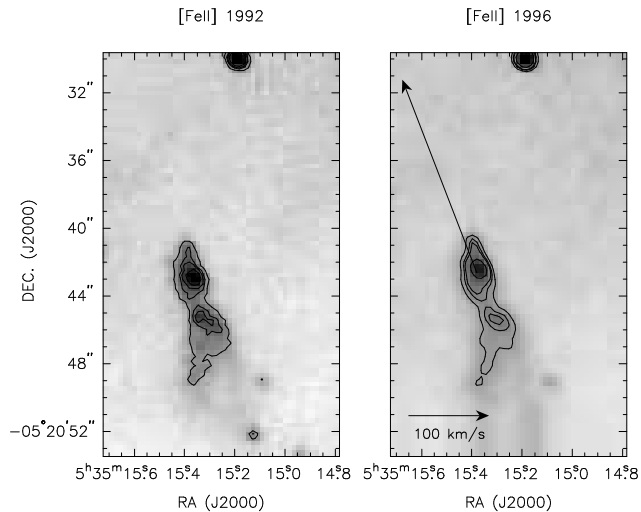


Figure 5. HH 154-041 (=HH 210, No. 27) is shown in [Fe II] line emission with the proper motion vector overlaid. Two or more bow features overlap here. While the overall shape is preserved, the lower emission peak has slightly shifted to the right, in comparison to the motion of the bullet head. The velocity vector and the scale bar, on right panel, are the same as in Figure 1.

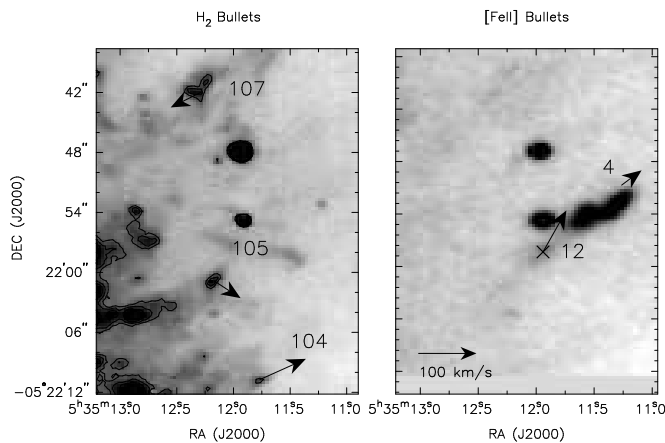


Figure 6. (left) Newly discovered H_2 bullets are shown with proper motion vectors overlaid as Figure 1. They are found between HH 113-156 (=HH 201, No. 4; right) and the presumed origin in the IRc2-complex. The corresponding [Fe II] line emission is shown right. The proper motion vector for HH 113-156 (No. 4) is offset for clarity, and the proper motion vector from the eye-estimation is used for HH 117-200 (No. 12; see text). The velocity vector and the scale bar, on right panel, are the same as in Figure 1.

is preserved the second emission peak shows a small shift ($0.6''$) to southwest, different from the northeast motion of the tip of the bullet.

3.2 Discovery of New H_2 Bullets

We report the discovery of new H_2 bullets; HH 117-212, HH 119-203 and HH 120-145 (Nos. 104, 105 and 107, respectively; Figure 6). They emit in H_2 only, located between HH 113-156 (=HH 201, No. 4) and the presumed origin

in the IRc2-complex. Their morphology resembles that of [Fe II] bullets but with smaller proper motions of order $\sim 100 \text{ km s}^{-1}$. We presume their slower speed results in a lower-excitation spectrum without [Fe II]. These are thus similar to the inner system of H_2 bullets discovered within 15 arcsec of IRc2-complex by Stolovy et al. (1998).

3.3 Noticeable Features in H_2 Line Emission

The proper motion measurements for both H_2 emitting wakes and H_2 bullets were difficult to determine because of their diffuse morphology. H_2 wakes which do have leading [Fe II] bullets appear to have a similar proper motion vector as their leading bullet. However, in general, the proper motions of H_2 bullets are slower than those of [Fe II] bullets.

HH 114-107, 115-055 & 115-103 [Nos. 101, 102 & 103]

HH 114-107 (No. 101) at the tip of HH 115-109/117-114 (Nos. 7/11) has no associated [Fe II] emission (Figure 3) and is found to be stationary. This may be a stationary cloudlet being rammed by the shock wave running ahead of the HH object, as is the case with the ‘tadpoles’ in Helix Nebula (eg. Burkert & O’Dell 1998). In such a case, the nearside of the clump to the IRc2-complex would show the highest excitation with its trail pointing away from the complex. Unfortunately the size of the knot is not big enough for such structure to be resolved.

The same explanation can be applied to 115-055 (No. 102) which is a bright triangle-shaped clump with a weak [Fe II] emission knot HH 117-057 (No. 10) interior to it. When their emission peaks in [Fe II] and H_2 are connected, the line has P.A. of $\sim 310^\circ$, pointing about 30 arcsec east of the IRc2-complex.

For 115-103 (No. 103), the emission peak has shifted to west by half an arcsecond giving much larger proper motion from eye-examination than from centroiding, as has its counterpart in [Fe II] emission HH 115-103 (No. 6).

120-120 [No. 106]

Two bow features are discernable in H_2 wakes associated with an emission peak at 120-120 (No. 106) (Figure 7). They are trailing the [Fe II] bullets HH 115-109 (No. 7) with P.A.= 330° and HH 117-114 (No. 11) with P.A.= 320° . A line, drawn along the presumed axis of the smaller bow feature, passes through a secondary [Fe II] emission peak at 118-119 which coincides with the tip of the bow. Extended further northwest, the line passes through HH 117-114 (No. 11). These features may arise from the fragmentation of the bullet into two pieces, rather than these being two separate bullets projected on top of one another.

Figure 7 also shows a morphological change at the head of these wakes. The cone-shaped tip of the H_2 wake in 1992 has disappeared leaving it flat-headed by 1996. Inhomogeneity in the ambient molecular cloud on scales of $\sim 100 \text{ AU}$, causing changes in the rate of entrainment of material behind a bullet, could produce such a change.

4 DISCUSSION

The most basic result from the data presented here is that the bullet/bow-shock interpretation placed on the observa-

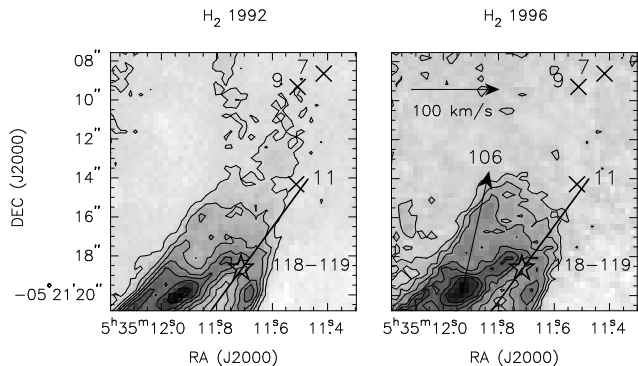


Figure 7. The open head of wakes accommodating H₂ clump 120-120 (No. 106), lead by the [Fe II] bullet system HH 115-109/HH 117-114 (Nos. 7/11). A straight line is drawn along the presumed axis of the smaller bow feature with P.A. of 320°. A star sign marks the position of a [Fe II] knot 118-119, and × the [Fe II] bullets HH 115-109 (No. 7), HH 116-110 (No. 9) and HH 117-114 (No. 11). The velocity vector and the scale bar in the right panel are the same as in Figure 1. See Figure 3 for the proper motion vectors for the [Fe II] bullets shown here.

tions of the [Fe II] caps and H₂ wakes in Orion by AB is essentially correct. The proper motions measured confirm that the bullets are travelling away from the core of the cloud at supersonic speeds, and are thus projectiles that are being shocked. They cannot be stationary cloudlets, nor can they be standing waves in a flow.

Their speeds, typically of order 200 km s⁻¹, and directions are consistent with both the widths of their line profiles, and with the morphology of individual bullets and fingers. We are observing bullets and associated wakes interacting with an ambient medium, spread over a wide opening angle, as they move outwards from the centre of the molecular cloud.

The inferred speeds are much in excess of the dissociation speeds for H₂ and even [Fe II], and thus cannot be the actual shock speed of the line emitting gas. There is, however, no suggestion from other data (eg. Tedds et al. 1999b) that the bullets are traversing a moving medium (thus reducing the shock velocity to the difference between the bullet and medium velocities). Oblique shocks, except at the very head, must occur with a significant tangential component of velocity remaining in the shocked material. This is as expected for a bow shock around a bullet, with only the normal component of the bullet’s motion at each point along the bow contributing to the shock speed.

We see little evidence for significant morphological changes in the bullets over the four-year baseline, nor for fading or brightening of individual knots over the same time, aside from [Fe II] clumps HH 112-109 and HH 130-119 (No. 20), and the head of the H₂ wake associated with 120-120 (No. 106) (see §3). This is thus different from the observation of some of the bullets in HH46/47 (?) and HH 111/121 (Coppin et al. 1998), where brightness variations on timescales of 1 year (the cooling time for H₂) are seen. Such variations likely arise from inhomogeneities in the ambient medium over spatial scales of at most some tens of AU, leading to changes in the amount of material being swept up over this time. For the bullets in Orion the medium must thus be reasonably homogeneous over ~ 100

AU scales, otherwise changes in shock strength, and thus line intensities, would be observed. However, the change in H₂ wake intensity near 120-120 (No. 106) and appearance of [Fe II] clump HH 112-109 (see Figure 3) suggests this region is not homogeneous over this scale. Here, a bullet may have fractured into several pieces, each forming its own set of H₂ wakes, overlapping behind. The similar transverse speeds of [Fe II] bullets HH 115-109, HH 116-110 and HH 117-114 (Nos. 7, 9 & 11) support this suggestion.

No differential motion, however, between [Fe II] bullets and their H₂ wakes is observed. While limits on such motion remain weak over a four year timescale, this suggests that the bullets are not separating from their wakes. Together with the lack of any morphological changes, the wakes also cannot be stretching. In other words, each bullet and wake appears to be moving together. This does not, however, imply that the gas within the bullet/wake is stationary with respect to the bullet velocity. Material swept-up by the bullet will be swept down the wake at the tangential component of the shock velocity, and will thus traverse the length of the bow. It will continue to be observed until it reaches the Mach point, where the normal component of the bullet velocity drops below the minimum shock speed to excite the gas (~ 5 km s⁻¹ for molecular gas). The time taken for this will be of order 100 years. Since the wakes are not stretching either, the bullets must also have been in motion for at least this long, in order to reach a steady-state configuration.

The bullets observed in H₂ only, on the inner edge of the finger system HH 113-156 (No. 4), are moving more slowly (~ 100 km s⁻¹) than those emitting in [Fe II] (~ 200 km s⁻¹), though their speeds still exceed that for dissociation of H₂. However, these slower speeds are consistent with lower excitation for the inner bullets, as would be inferred by the absence of [Fe II] in them. This gives support to the inner H₂ bullet system discovered by Stolovy et al. (1998) within 15 arcsec of IRc2-complex as being slower moving analogues of the [Fe II] bullets.

Nevertheless not all line-emitting knots are moving outwards at these speeds. For instance, HH 117-057 (No. 10) and 115-055 (No. 102) appears to be stationary with respect to the ambient cloud. HH 114-107 (No. 101) is also stationary with HH 115-109/HH 117-114 (Nos. 7/11) moving towards it. We hypothesise that it is a dense clump in the ambient medium just now being rammed by HH 115-109/HH 117-114 (Nos. 7/11). Time variability is evident in [Fe II] clump, HH 112-109 in Figure 3, which showed up in 1996 but was not seen in 1992. In all these cases, we expect the clumps to brighten over the next few years as they are further overrun.

The proper motion vectors of the bullets clearly extend back towards an origin somewhere in the vicinity of IRc2-complex. However their extrapolation remains no more accurate than that undertaken by Allen & Burton (1993), who extended the wakes back towards an origin within 5 arcsec of the IRc2-complex. Our present data still cannot shed any more light on where this might be, which awaits a longer time baseline of measurements.

The projected distance of bullets from IRc2-complex is plotted against its proper motion speed in Figure 8. Excluding HH 130-119 (No. 20) which was problematic in its measurement, the plot suggests that more distant bullets, in general, are moving faster. This is consistent with an explosive, or at least an impulsive event, as the origin for the

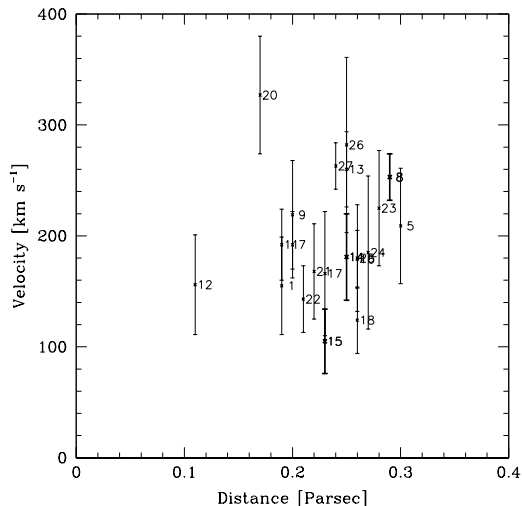


Figure 8. The bullet speeds whose $S/N \geq 3$ are plotted against their projected distance from the IRC2-complex, again numbered with those in the first column of Table 1. Thick solid lines are for HH 116-025 (No. 8), 122-041 (No. 14) and 125-053 (No. 15) from right to left (see §4).

bullets. Certainly it must have occurred over a timescale much less than that of the expansion, i.e. $\ll 1,000$ years. This is most clearly demonstrated for HH 125-053, 122-041 and 116-025 (No. 8, 14 and 15, respectively) along the main finger, which show a linear increase in speed with distance. However the motions are not consistent with free expansion from the IRC2-complex; extrapolation to zero speed would suggest an origin $0.05 - 0.1$ pc from the IRC2-complex. This might correspond to where the bullets have formed, through instabilities in a time variable wind.

5 FUTURE WORK

Our data represent just two epochs of observation, and is only the start of an investigation of the motion of the Orion bullets. With further epochs of data we will be able to address further questions regarding their origin and excitation, including:

- (a) whether the bullets are decelerating (changing in velocity)?
- (b) are there non-radial motions, perhaps imparted by collisions with dense objects?
- (c) are there more differential motions between the bullets and their wakes?
- (d) could we be seeing a pattern speed of a bullet, rather than its bulk motion? This may be evident if wiggles are observed on a proper motion vector.
- (e) are there more morphological or intensity changes in time, such as the stretching of a wake or the brightening or fading of a knot? These might arise from inhomogeneities in the ambient medium, thus indicating what scale these occur on.

Further proper motion vectors will help tie down the origin of the driving source, by reducing the errors on their extrapolation back to an origin. Combining the data with line profile measurements would give the 3D velocity of a

bullet, and allow a 3D picture of their distribution in space to be built up. The line profiles could then be compared to models such as those of Hartigan et al. (1987) which predict profile shapes for a range of orientation angles. In addition, determining an orientation directly will help constrain shock models for the line production, such as the form of the cooling law and shape of the bow, which significantly effect the resultant profile. The [FeII] data can also be compared to optical data obtained with HST, which should yield more accurate velocities on shorter time base lines due to the superior spatial resolution that can be obtained.

ACKNOWLEDGMENTS

We would like to thank Dr. J. A. Tedds for providing line profile information for some of bullets studied here. This project is partly funded by research grants from the ‘Small Grants’ scheme of the Australian Research Council (ARC).

REFERENCES

- Allen D. A. et al., 1993, Proc. Astron. Soc. Aust., 10, 298
 Allen D. A., Burton M. G., 1993, Nat, 363, 54 (AB)
 Axon D., Taylor K., 1984, MNRAS, 207, 241
 Burkert A., O’Dell C. R., 1998, ApJ, 503, 792
 Coppin K. E., Davis C., Micono M., 1998, MNRAS, 310, L10
 Genzel R., Stutzki J., 1989, ARA&A, 27, 41
 Hartigan P., Raymond J., Hartmann L., 1987, ApJ, 316, 323
 Hu X., 1996, AJ, 112, 2712
 Jones B. F., Walker M. F., 1985, AJ, 90, 1320
 Micono M., Davis C. J., Ray T. P., Eisloffel J., Shetrone M. D., 1998, ApJ, 494, L227
 O’Dell C. R., Wen Z., 1994, ApJ, 436, 194
 O’Dell C. R., Wong S. K., 1996, AJ, 111, 846
 Prosser C. F., Stauffer J. R., Hartmann L., Soderblom D. R., Jones B. F., Werner M. W., McCaughrean M. J., 1994, ApJ, 421, 517
 Reipurth B., 1999, A general catalogue of Herbig-Haro objects. 2nd edition, <http://casa.colorado.edu/hhcat>
 Stolovy S. et al., 1998, ApJ, 492, 151
 Stone J., Xu J., Mundy L., 1995, Nat, 377, 315
 Tedds J. A., Brand P. W. J. L., Burton M. G., 1999a, MNRAS, 307, 337
 Tedds J. A., Brand P. W. J. L., Burton M. G., 1999b, MNRAS, in preparation

Table 1. Proper Motions of the Orion Bullets and Wakes in [Fe II] and H₂ emission.

No.	Bullet Designation	μ^1 ($''$ /cent.)	v_{tan}^2 (km s ⁻¹)	This study			Previous studies		Remark
				P.A. ³ (deg)	μ^4 ($''$ /cent.)	μ^5 ($''$ /cent.)	v_{tan}^2 , P.A. ³ (km s ⁻¹ , deg)	v_s , O.A. ⁶ (km s ⁻¹ , deg)	
[Fe II] knots									
1	HH 103-128	7.2 ± 2.1	155 ± 44	342 ± 16	6.4	6.4 ± 0.4			
2	HH 109-148	1.6 ± 2.4	34 ± 51	293 ± 56	1.9	8.0 ± 0.4			
3	HH 113-136	5.1 ± 2.0	110 ± 43	132 ± 21	3.1	7.2 ± 0.4			
4	HH 113-156	1.8 ± 1.0	38 ± 21	297 ± 29	8.4	4.9 ± 0.4	170, 324 ^a 167, 304 ^b	310, 15 ^a	HH 201
5	HH 114-023	9.8 ± 2.4	209 ± 52	339 ± 14	10.2	8.5 ± 0.4			
6	HH 115-103	4.6 ± 3.2	99 ± 69	257 ± 35	2.1	7.7 ± 0.4			
7	HH 115-109	9.0 ± 1.4	192 ± 30	326 ± 09	8.5	8.6 ± 0.4			HH 120-114 ^c
8	HH 116-025	11.8 ± 1.0	253 ± 21	354 ± 05	10.1	9.2 ± 0.4	253, 343 ^a 236, 344 ^b	120, 90 ^a	HH 205
9	HH 116-110	10.3 ± 2.3	219 ± 49	335 ± 13	8.8	12.0 ± 0.4			
10	HH 117-057	3.4 ± 3.2	72 ± 68	213 ± 43	2.3	4.5 ± 0.4			
11	HH 117-114	9.0 ± 1.5	192 ± 32	321 ± 09	6.3	10.0 ± 0.4		120, 60 ^c	HH 120-114 ^c
*12	HH 117-200	7.3 ± 2.1	156 ± 45	31 ± 16	10.0	4.2 ± 0.4			
13	HH 121-041	12.2 ± 1.6	260 ± 34	334 ± 08	12.0	9.8 ± 0.4			
14	HH 122-041	8.5 ± 1.8	181 ± 39	341 ± 12	7.9	12.4 ± 0.4	251, 333 ^a		HH 206
15	HH 125-053	4.9 ± 1.3	105 ± 29	332 ± 15	4.3	3.6 ± 0.4		150, 70 ^c	HH 207 HH 126-053 ^c
16	HH 128-037	8.4 ± 1.2	179 ± 26	352 ± 08	8.4	11.3 ± 0.4			
17	HH 128-048	7.7 ± 2.6	166 ± 56	0 ± 19	6.1	6.3 ± 0.4			
18	HH 130-036	5.8 ± 1.4	124 ± 30	17 ± 13	3.7	2.7 ± 0.4			
19	HH 130-041	1.6 ± 1.6	34 ± 34	254 ± 45	2.3	6.3 ± 0.4			
*20	HH 130-119	15.3 ± 2.5	327 ± 53	125 ± 09	5.6	6.6 ± 0.4			
21	HH 133-054	7.9 ± 2.0	168 ± 43	308 ± 14	3.7	7.2 ± 0.4			
22	HH 133-056	6.7 ± 1.4	143 ± 30	330 ± 12	4.5	6.8 ± 0.4			
23	HH 138-026	10.6 ± 2.5	225 ± 52	350 ± 13	6.9	7.6 ± 0.4			
24	HH 139-035	8.4 ± 2.2	180 ± 48	349 ± 15	6.9	12.6 ± 0.4			
25	HH 140-029	8.6 ± 3.2	185 ± 69	350 ± 20	8.4	7.7 ± 0.4			
26	HH 140-037	13.2 ± 3.7	282 ± 79	12 ± 16	11.9	7.0 ± 0.4			
27	HH 154-041	12.3 ± 1.0	263 ± 21	21 ± 05	8.4	7.0 ± 0.4	215, 16 ^b	400, 0 ^a	HH 210
H₂ knots									
101	HH 114-107	0.8 ± 1.6	17 ± 33	337 ± 62	1.7	0.0 ± 0.4			stationary
102	115-055	1.3 ± 1.1	27 ± 24	267 ± 41	3.3	2.4 ± 0.4			stationary?#
103	115-103	4.7 ± 1.8	100 ± 39	267 ± 21	5.4	12.6 ± 0.4			
104	HH 117-212	4.2 ± 0.7	89 ± 15	333 ± 10	2.5	5.1 ± 0.4			New bullet
105	HH 119-203	2.7 ± 0.7	57 ± 15	233 ± 15	3.3	3.3 ± 0.4			New bullet
106	120-120	6.3 ± 1.5	135 ± 32	347 ± 13	4.2	8.6 ± 0.4			
107	HH 120-145	2.8 ± 0.9	60 ± 19	150 ± 17	0.4	0.7 ± 0.4			New bullet
108	124-055	3.1 ± 1.7	66 ± 36	299 ± 29		11.6 ± 0.4			
109	126-054	5.6 ± 1.8	119 ± 39	304 ± 18	7.0	9.8 ± 0.4			
110	128-113	4.1 ± 1.2	88 ± 25	18 ± 16		5.7 ± 0.4			
111	130-119	2.7 ± 0.8	57 ± 17	319 ± 17	0.4	0.3 ± 0.4			

The proper motion of bullets in [Fe II] is followed by the proper motion of bullets and wakes in H₂ (from No. 101 to 111). In naming H₂ knots, HH indicating Herbig–Haro object is only given when it is an H₂ bullet, and not when it is the wake behind an [Fe II] bullet.

¹ From the shift in the intensity centroids of a bullet in two epochs. A proper motion of 10 arcsec per century corresponds to a transverse speed of 215 km s⁻¹ at the distance of 450 pc to OMC-1.

² The tangential velocity; the velocity projected onto the plane-of-sky.

³ The position angle; the direction of motion in the plane-of-sky, starting from N and increasing to E.

⁴ From the cross-correlation of the distribution of emission from the bullets at two epochs. It generally agrees with the results from the centroid (see §2). The diffuse shape of H₂ knots sometimes makes cross-correlation unreliable, when their value is not given.

⁵ From eye-estimation of the contour maps of bullets. Eye-estimation is sensitive to changes in the intensity peak only.

⁶ The shock velocity and orientation angle. The shock velocities are estimated from the line profile of [O I] (Hu 1996) and [Fe II] (Tedds et al. 1999a). The orientation angle is the angle between our line-of-sight and the direction of motion of an object. O.A.=90° when the object is moving on the plane-of-sky.

* For these bullets, the proper motion vectors from the eye-estimation (P.A.=333° for No. 12 and 5° for No. 20, respectively) are used in Figure 1 (see text).

See §3.2 for the discrepancy in the proper motion values from different methods.

(a) Hu (1996), d=440 pc used; (b) Jones & Walker (1985), d=460 pc used; (c) Tedds et al. (1999a)